Detection of Liver Metastases from Pancreatic Cancer Using FDG PET

Andrea Fröhlich, Christoph G. Diederichs, Ludger Staib, Jochen Vogel, Hans G. Beger and Sven N. Reske

Departments of Nuclear Medicine, Surgery and Diagnostic Radiology, University Hospital of Ulm, Ulm, Germany

We evaluated the potential of the glucose analog [^{18}F]fluorodeoxy-glucose (FDG) as a PET tracer for the hepatic staging in 168 patients designated for resective pancreatic surgery. **Methods:** Metastatic liver disease was confirmed or excluded during surgery or with CT follow-up for at least 6 mo. Proven metastases were then retrospectively identified on preoperative CT (gold standard). Hepatic PET scans of all patients were interpreted blindly. Any focal FDG uptake was considered malignant. Both proven hepatic metastases and suspicious hepatic PET lesions were then compared, lesion by lesion, with CT. Standardized uptake values (SUV) and tumor-to-liver ratios (T/L) were determined for the most intense lesion of each patient. **Results:** Sensitivity of FDG PET was 68% (15 of 22 patients). The lesion detection rate was 97% (28 of 29 metastases) for lesions >1 cm and 43% (16 of 37 metastases) for lesions ≤1 cm. Specificity was 95% (138 of 146 patients). Six of eight patients with false-positive results had marked intrahepatic cholestasis (versus 3 of 15 patients with true-positive lesions), one had an infrahepatic abscess and one had a right basal pulmonary metastasis. The SUV and T/L were 4.6 ± 1.4 and 2.3 ± 1.1, respectively, for malignant lesions and 4.1 ± 1.5 and 1.9 ± 0.3, respectively, for false-positive lesions and therefore are of limited value. **Conclusion:** FDG PET provides reliable hepatic staging for lesions >1 cm. False-positive results are associated with the presence of marked intrahepatic cholestasis. For lesions ≤1 cm, FDG PET can define malignancy in 43% of suspicious CT lesions in the absence of dilated bile ducts.

Key Words: FDG PET; pancreatic cancer; liver metastases

J Nucl Med 1999; 40:250–255

T he prognosis for pancreatic carcinoma is poor. In 70% of patients who undergo pancreatectomy, occult liver metastases that may already have existed at the time of surgery are one of the most common sites of treatment failure (1–3). Surgery is considered the only curative therapy. However, once hepatic metastases are present, a curative resection is not possible. Conservative attempts to improve survival include radiochemotherapy. Novel experimental therapeutic strategies include gene therapy, immunotherapy and antisenese oligonucleotides (4).

The incidence of chemo- or radio-resistant tumor cells as

a consequence of cellular mutations rises sharply with increased tumor volume (5). The tumoral growth fraction is at maximum for tumor cell numbers of 10^5-10^8 tumor cells, which equals 1 mg to 1 g of tumor tissue (6). These data emphasize the necessity of detecting small, fast-growing tumor manifestations. Early detection of small tumor manifestations might provide the chance to improve conservative treatment for this usually fatal disease. Also, careful hepatic evaluation continues to be vital for the proper selection of patients who are potential operative candidates.

Spiral CT, performed during the peak level of hepatic parenchymal enhancement, is considered the mainstay of noninvasive hepatic staging (7). However, smaller liver nodules (<1 cm) are frequently missed (8–10). This was found to be the most common reason for inaccurate preoperative assessment with spiral CT (8,10,11). MRI may be more sensitive than standard CT techniques (12), but patient numbers in published studies are small and some authors doubt its advantages over CT (13,14). Intraoperative ultrasound is considered the most sensitive technique for metastatic detection. However, it lacks specificity and is applicable only to patients who already have been selected for operative procedures (15). Other limitations are the detection of superficially located lesions, the presence of focal nonsteatosis and the differentiation of hyperechogenic metastases from hemangioma (16). CT during arterial portography (CTAP) is considered equally sensitive as intraoperative ultrasound; sensitivity values approach 90% (17,18). However, it requires arterial angiography and its specificity is low because of a high prevalence of false-positive findings caused by focal hepatic parenchymal perfusion defects (19,20).

Approximately 50% of lesions ≤15 mm in diameter in CT are benign (21). Because lesions of this size may be difficult to differentiate from malignant lesions with anatomically based imaging techniques, a more specific method should improve diagnostic accuracy.

Functional imaging not only may provide additional information based on biochemical alterations in tissue increasing the specificity of the diagnostic work-up but also may detect lesions in the absence of anatomical changes. The glucose analog [^{18}F]fluorodeoxyglucose (FDG) is the most common PET tracer used in oncology. Because of its metabolic characteristics, FDG is trapped in tissues with increased glucose metabolism (22), a common metabolic

feature of many solid malignancies, including cancer of the pancreas (23–25).

It has been shown that FDG accumulates in liver metastases from colorectal carcinoma (26) and that FDG PET can be used for liver staging (27). PET appears useful, selecting patients with apparently curable colorectal cancer metastases to the liver for hepatic resection (28). Other observers have demonstrated the ability of PET to monitor changes in metabolism of hepatic lesions during chemotherapy (29–31).

Only preliminary reports about the hepatic staging of pancreatic carcinoma with PET were available (23–25). Therefore, we evaluated the ability of FDG PET to detect hepatic metastases in patients scheduled for pancreatic surgery. We correlated our findings with CT follow-up or intraoperative findings. We sorted our results according to lesion size and identified reasons for false-positive FDG PET results.

MATERIALS AND METHODS

Patient Population

Between April 1992 and August 1995, a total of 189 consecutive patients designated for resective pancreatic surgery received abdominal PET. Twenty-one patients were excluded because hepatic status could not be obtained because of incomplete follow-up data. Of the remaining 168 patients (95 men, 73 women; median age 56 ± 13 y), 94 had pancreatic carcinoma and 74 had benign pancreatic disease.

Computed Tomography. Contrast-enhanced CT scans were obtained in various institutions to identify hepatic metastases. Because of limited availability, only 12% were the spiral technique. In general, contiguous sections 8- to 10-mm thick were obtained, before and during rapid intravenous injection of about 100 mL of a 60% iodinated contrast agent.

PET. PET was performed by using a commercially available scanner (ECAT 931–08–12; CTI Siemens, Knoxville, TN) that allows simultaneous acquisition of 15 contiguous slices in one bed position. Primary and secondary slices were 6.75-mm thick. Patients fasted for at least 12 h before the study. Transmission imaging for attenuation correction was performed before emission scans with a [67]Ge/^{68}Ga ring source in at least three bed positions, starting at the liver dome. Acquisition time was 10 min per bed position.

FDG was synthesized according to standard procedures (32). Furosemide (20 mg) was injected intravenously to reduce artifacts due to high radioactivity in the renal collecting system. About 1 h after intravenous injection of 270–370 MBq (7–10 mCi) FDG, the patient was repositioned with laser-guided landmarks and the recording emission scans were begun. Images were reconstructed with an iterative reconstruction algorithm (33).

Image Interpretation

All CT scans were interpreted at each institution by experienced radiologists. One of the authors retrospectively analyzed patient images that showed intrahepatic lesions at the initial scan or during the follow-up period and had other evidence of hepatic involvement (e.g., intraoperative findings). Any liver lesion was reported by localization and size. Hepatic status at the time of PET scanning was determined in awareness of clinical and CT follow-up.

All PET studies were retrospectively re-interpreted with respect to the presence and location of hepatic lesions. This was done by another author, blinded to other imaging tests or clinical data except pancreatic lesion of unknown nature. Transversal, coronal and sagittal slices were viewed with varying image normalization on the workstation's screen with standard ECAT 6.0 software. Any focal increased FDG uptake was considered malignant.

For quantitative interpretation, a region of interest (ROI) analysis was performed in all patients who presented suspicious hepatic PET lesions. A circular ROI, 1 cm in diameter, was placed over the most intense lesion of each patient. A second ROI, 3.1 cm in diameter, was placed over normal liver tissue. The ROI data were processed in two ways: as a standarized uptake value (SUV; activity concentration ÷ injected dose/body weight) and as a tumor-to-normal liver ratio (T/L).

Data Analysis

Metastatic involvement of the liver at the time of pancreatectomy was confirmed or excluded by CT follow-up over a period of at least 6 mo and by combined intraoperative hepatic palpation with biopsy of suspicious lesions, if possible. During CT follow-up, malignancy was considered proven if lesions grew more numerous or larger in diameter. All lesions identified during the follow-up period were traced back to the time of pancreatectomy. Therefore, even small lesions (3–10 mm) could be positively identified as malignant in the preoperative CT. Metastatic disease was ruled out in patients who did not show any new or progressive lesions during the follow-up period.

All proven hepatic metastases and all suspicious hepatic PET lesions were compared with the corresponding preoperative CT, lesion by lesion. Results were sorted according to lesion size. All metastases that were not detected by PET were considered false-negatives and all PET lesions in patients without malignant liver disease were considered false-positives.

RESULTS

Twenty-four patients were determined to have metastatic liver disease. In 2 patients, the PET study was technically inadequate (liver not completely imaged) and thus was excluded from the study. The remaining 22 patients are listed in Table 1.

Ten patients were found to have metastatic liver disease at combined surgical and histopathologic examination. In 12 patients, confirmation of hepatic involvement was obtained by CT follow-up. A total of 66 malignant lesions were found. The mean number of hepatic metastases per patient was three (range 1–10). The mean diameter of the lesions was 1.3 cm (range 0.3–4 cm).

Sensitivity of FDG PET was 68% (15 of 22 patients). The lesion detection rate was 97% (28 of 29 metastases) for lesions >1 cm and 43% (16 of 37 metastases) for lesions ≤1 cm. Specificity was 95% (138 of 145 patients). Figure 1 illustrates a small intrahepatic metastasis that clearly shows focally increased FDG accumulation. In 8 patients, PET provided false-positive results (Table 2). Six of these patients had marked intrahepatic cholestasis (Fig. 2), versus 3 of 15 patients with true-positive lesions; 1 had an infrahepatic abscess and 1 had a right basal pulmonary metastasis. PET failed to show metastatic hepatic lesions

TABLE 1
Patient and Lesion Characteristics in 22 Patients with Confirmed Liver Metastases of Pancreatic Cancer

Patient no.	Sex	Age (y)	Range of lesion Size (cm)	Lesion detection rate ≤1 cm	Lesion detection rate >1 cm	SUV	T/L	Patient detection
1	F	66	0.8	0/1	—	—	—	FN
2	M	51	0.5–1.0	0/3	—	—	—	FN
3	M	64	0.9–1.2	4/4	2/2	5.5	2.6	TP
4	M	39	0.5–2.5	2/7	2/2	3.1	1.9	TP
5	M	69	0.5	1/1	—	3.8	1.4	TP
6	F	75	0.5–1.3	0/2	0/1	—	—	FN
7	M	65	0.5	0/1	—	—	—	FN
8	M	67	4.0	—	1/1	3.8	1.6	TP
9	F	55	2.0	—	1/1	3.3	1.7	TP
10	M	37	1.5	—	1/1	7.6	5.7	TP
11	M	62	1.0	0/1	—	—	—	FN
12	M	46	0.5–3	2/2	3/3	4.2	2.5	TP
13	F	56	0.5–1.3	2/2	1/1	6.0	2.8	TP
14	M	60	2.2	—	1/1	4.2	3.0	TP
15	M	66	1–1.5	1/2	3/3	4.5	1.9	TP
16	F	48	0.3–4	0/3	7/7	4.4	2.4	TP
17	M	75	0.3	0/1	—	—	—	FN
18	M	51	0.8–2.0	0/2	3/3	7.3	2.3	TP
19	M	53	0.5–1.0	3/3	2/2	3.5	1.6	TP
20	M	52	0.5	1/1	—	3.5	1.4	TP
21	F	69	1.0	0/1	—	—	—	FN
22	M	71	5.0	—	1/1	4.0	2.3	TP
				16/37	28/29	4.6 ± 1.4	2.3 ± 1.1	15/22

— = not applicable; FN = false-negative; TP = true-positive.
Standardized uptake value (SUV) and tumor-to-liver ratio (T/L) were calculated for the most intense lesion of each patient.

with 7 patients (false-negatives). The calculated SUV and T/L ratio were 4.6 ± 1.4 and 2.3 ± 1.1, respectively, for malignant lesions and 4.1 ± 1.5 and 1.9 ± 0.3, respectively, for benign lesions (Fig. 3).

DISCUSSION

FDG PET provides reliable hepatic staging for lesions >1 cm but for smaller lesions, sensitivity is limited. However, in the absence of intrahepatic cholestasis, specificity reaches values near 100%, even in small lesions. This finding may be of considerable significance when few or single lesions cannot reliably be graded malignant or benign with a morphological method. Alternatively, equivocal CT findings might be verified by MRI (which is highly accurate in detecting cysts or hemangiomas) or laparoscopic techniques (i.e., direct visualization and histologic examination). These alternatives warrant further studies.

According to studies concerning liver staging in patients with colorectal carcinoma, the sensitivity of FDG PET is 90%–97%, with a specificity ranging from 88% to 100% (24,25,34,35). The observed supposedly lower sensitivity for PET found in our study does reflect the lower sensitivity for small lesions ≤1 cm (Table 1). In agreement with our findings, Vitola et al. (27) reported that of four malignant lesions measuring <1 cm, two were seen and two were missed with PET. The mean diameter of the lesions was 3 ±

2 cm, which is much larger than our lesions (Table 1). Other authors did not report lesion size. Therefore, our results are not necessarily different from previous findings if lesion sizes are considered.

In our study, one metastasis >1 cm was not detected. This patient presented multilocular peritoneal metastases diagnosed with PET. The liver lesion was located near the liver surface and was erroneously considered peritoneal.

The limited sensitivity of FDG PET for small lesions may have several causes: the activity in small lesions is underestimated because of the partial volume effect, but this underestimation could be reduced by improving the spatial resolution of PET; movement artifacts may be reduced by breath gating of the measurement and by avoiding reintroduction of the patient to the scanner; the high physiological FDG uptake of the liver (background) obscures lesions (36); some lesions may have a low glucose avidity; timing for data acquisition after FDG administration may not be optimal; patient fasting may be too short and lead to an unnecessary high liver FDG uptake; and the duration of imaging may be too short.

A general limitation of this study is the "gold standard" used. The most accepted standard is still provided by invasive procedures such as intraoperative ultrasound combined with direct surgical examination and biopsy of the liver. In our study, verification was obtained in 10 cases from
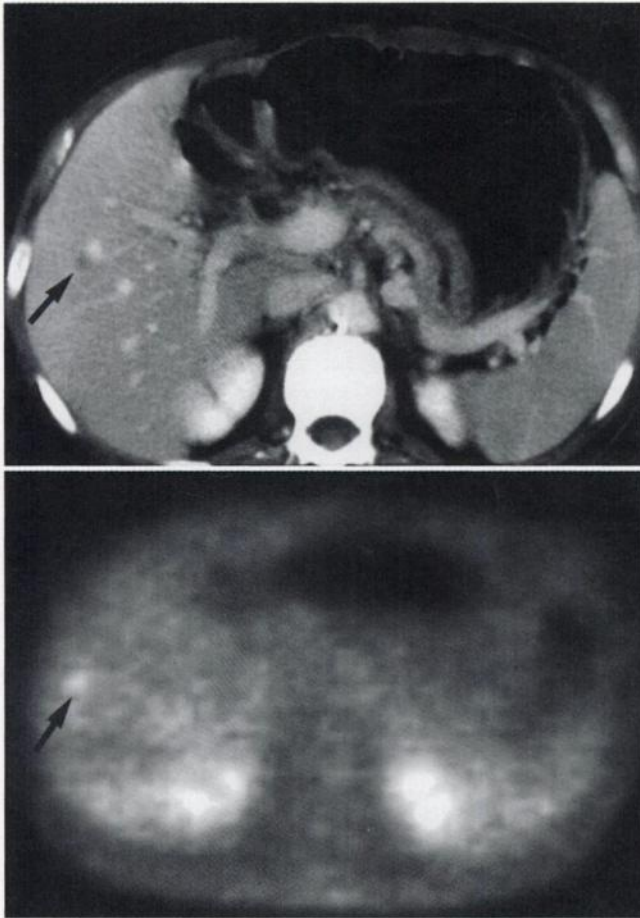
FIGURE 1. CT (top) and PET (bottom) images of patient with pancreatic carcinoma. Small intrahepatic metastasis is evident (arrow).
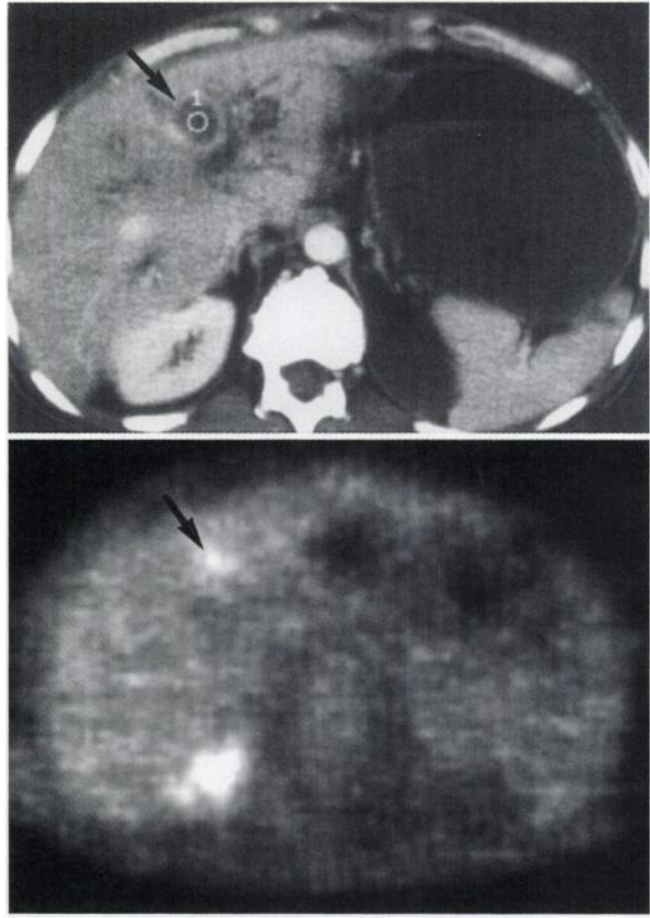

FIGURE 2. CT (top) and PET (bottom) images of false-positive patient with marked intrahepatic cholestasis. Focally increased FDG uptake, suggestive of metastasis, is evident. On CT scan, region-of-interest circle is drawn into one of dilated bile ducts.

TABLE 2
Characteristics of 8 Patients with
False-Positive PET Findings

Patient no.	Sex	Age (y)	Diagnosis	Number of lesions	SUV	T/L
23	F	51	Right basal pulmonary metastasis	1	5.7	2.4
24	M	49	Cholestasis	2	2.6	1.7
25	M	63	Cholestasis	8	2.6	1.5
26	M	53	Cholestasis	1	5.2	2.3
27	M	53	Subhepatic abscess	1	3.0	1.8
28	M	69	Cholestasis	1	3.0	2.1
29	M	55	Cholestasis	2	6.0	2.0
30	F	81	Cholestasis	1	5.0	1.6
Average					4.1 ± 1.5	1.9 ± 0.3

Standardized uptake value (SUV) and tumor-to-liver ratio (T/L) were calculated for the most intense lesion of each patient. Cholestasis was diagnosed by CT by dilating intrahepatic bile ducts to >3 mm at the level of second-degree portal branches.
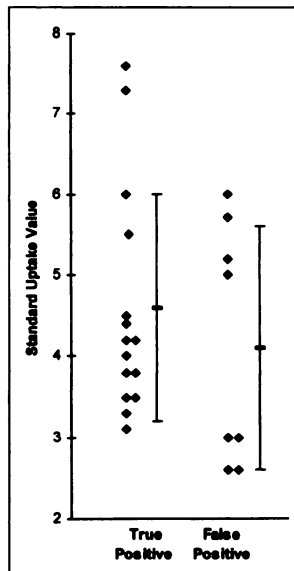

FIGURE 3. SUVs. Calculated mean ± SD is given for most intense lesion in each patient.

histologic examination of the lesions. The other 12 were verified by a CT follow-up. Only a few CT scans (12%) were performed with the spiral technique. Additionally, the scans were of varying quality because they were performed at different institutions. Advanced CT techniques (e.g., dual-phase helical CT) and/or MRI techniques (dynamic MRI with gadolinium or newer contrast agents for liver) might have revealed more lesions. Therefore, the lesion detection rate for small lesions and patient sensitivity may have been overestimated in our study.

False-positive results were found in eight patients. In one patient, a right basal pulmonary metastasis could not be differentiated from a hepatic lesion and another patient had a subhepatic abscess. The other six patients had marked intrahepatic cholestasis (Fig. 3). Intrahepatic cholestasis may lead to inflammatory reactions or abscesses in the bile duct system. It is well known that FDG accumulates in infectious processes, activated immunocompetent cells and granulation tissue (37,38). Therefore, positive PET scans of patients with suspected concomitant infectious processes or with marked intrahepatic cholestasis should be interpreted with caution.

Quantitative evaluation was performed for all suspicious hepatic PET lesions. No significant difference in the SUVs or T/L between benign (false-positive) and malignant lesions could be found. This result might be attributed to the fact that only lesions that have been considered malignant by visual image interpretation have been quantified. We did not measure any other benign lesions—such as cysts or hemangioma—because they obviously had no focally increased FDG uptake.

PET provides a method that is based not on morphological but primarily on functional tissue characteristics. Therefore, in the context of this study, PET is complementary to CT by adding specific information concerning the nature of the lesions. The combination of CT and PET could have resulted in accurate classification of liver metastases in 43% of CT lesions that were ≤1 cm 3–6 mo before definite diagnosis of metastatic disease to the liver.

CONCLUSION

The results of this study indicate that for lesions >1 cm, PET detects nearly all metastases in the absence of intrahepatic cholestasis. For lesions ≤1 cm, PET allows the confirmation of malignancy in about one-half of the lesions that are frequently of indeterminate nature according to morphological based imaging tests. The combination of both imaging modalities may be superior to the single techniques. For small lesions, a negative PET scan is of no value.

REFERENCES

1. Amikura K, Kobari M, Matsumo S. The time of occurrence of liver metastasis in carcinoma of the pancreas. *Int J Pancreat.* 1995;17:139–146.
2. Gilbert HA, Kagan AR. Metastases: incidence, detection, and evaluation without histologic confirmation. In: Weiss L, ed. *Fundamental Aspects of Metastasis.* Amsterdam, The Netherlands: North-Holland; 1976:385–405.
3. Kemeni N, Sugarbaker PH. Treatment of metastatic cancer to liver. In: DeVita VC, Hellman S, Rosenberg SA, eds. *Cancer, Principles and Practice of Oncology.* 3rd ed. Philadelphia, PA: JB Lippincott; 1989:2275–2298.
4. Clark JW, Glicksman AS, Wanebo HJ. Systemic and adjuvant therapy for patients with pancreatic carcinoma. *Cancer.* 1996;78(suppl):688–693.
5. Goldie JH. Scientific basis for adjuvant and primary (neoadjuvant) chemotherapy. *Semin Oncol.* 1987;14:1–7
6. Norton L, Simon R. Tumor size, sensitivity to therapy, and design of treatment schedules. *Cancer Treat Rep.* 1977;61:1307–1317.
7. Baker ME, Pelley R. Hepatic metastases: basic principles and implications for radiologists. *Radiology.* 1995;197:329–337.
8. Bluemke DA, Cameron JL, Hruban RH, et al. Potentially resectable pancreatic adenocarcinoma: spiral CT assessment with surgical and pathologic correlation. *Radiology.* 1995;197:381–385.
9. Brambs HJ, Claussen CD. Pancreatic and ampullary carcinoma. Ultrasound, computed tomography, magnetic resonance imaging and angiography. *Endoscopy.* 1993;25:58–68.
10. Diehl SJ, Lehmann KJ, Sadick M, et al. Pancreatic cancer: Value of dual-phase helical CT in assessing resectability. *Radiology.* 1998;206:373–378.
11. Warshaw AL, Tepper JE, Shipley WU. Laparoscopy in the staging and planning for pancreatic cancer. *Am J Surg.* 1986;151:76–80.
12. Bennett WF, Bova JG. Review of hepatic imaging and a problem-oriented approach to liver masses. *Hepatology.* 1990;12:761–775.
13. Wernecke K, Rummeny E, Bongartz G, et al. Detection of hepatic masses in patients with carcinoma: comparative sensitivities of sonography, CT, and MR imaging. *AJR.* 1991;157:731–739.
14. Zerhouni EA, Rutter C, Hamilton SR, et al. CT and MR imaging in the staging of colorectal carcinoma: report of the Radiology Diagnostic Oncology Group II. *Radiology.* 1996;200:443–451.
15. Rummeny EJ, Reimer P, Daldrup H, Peters PE. Detektion von Lebertumoren. *Radiologe.* 1995;35:252–258.
16. Meijer S, Paul MA, Cuesta MA, Blomjous J. Intra-operative ultrasound in detection of liver metastases. *Eur J Cancer.* 1995;31A:1210–1211.
17. Soyer P, Levesque M, Elias D, Zeitoun G, Roche A. Detection of liver metastases from colorectal cancer: comparison of intraoperative US and CT during arterial portography. *Radiology.* 1992;183:541–544.
18. Small WC, Mehard WB, Langmo LS, et al. Preoperative determination of the resectability of hepatic tumors: efficacy of CT during arterial portography. *AJR.* 1993;161:319–322.
19. Peterson MS, Baron RL, Dodd GD III, et al. Hepatic parenchymal perfusion defects detected with CTAP: imaging-pathologic correlation. *Radiology.* 1992;185:149–155.
20. Soyer P, Lacheheb D, Levesque M. False-positive CT portography: correlation with pathologic findings. *AJR.* 1993;160:285–289.
21. Urban BA, Fishman EK, Kuhlman JE, Kawashima A, Hennessey JG, Siegelman SS. Detection of focal hepatic lesions with spiral CT: comparison of 4- and 8-mm interscan spacing. *AJR.* 1993;160:783–785.
22. Warburg O. *The Metabolism of Tumors.* New York, NY: Richard R. Smith, Inc.; 1931:129–169.
23. Bares R, Dohmen BM, Cremerius U, Fass J, Teusch M, Büll U. Ergebnisse der Positronenemisionstomographie mit Fluor-18-markierter Fluordesoxyglukose bei Differentialdiagnose und Staging des Pankreaskarzinoms. *Radiologe.* 1996;36:435–440.
24. Friess H, Langhans J, Ebert M, et al. Diagnosis of pancreatic cancer by 2-[18F]-fluoro-2-deoxy-D-glucose positron emission tomography. *Gut.* 1995;36:771–777.
25. Stollfuss JC, Grillenberger KG, Fries H, et al. Pathophysiological basis and clinical value of 18F-fluorodeoxyglucose and positron emission tomography in pancreatic adenocarcinoma. *Dig Surg.* 1994;11:360–365.
26. Yonekura Y, Benua RS, Brill AB, et al. Increased accumulation of 2-deoxy-2-[18F]fluoro-D-glucose in liver metastases from colon carcinoma. *J Nucl Med.* 1982;23:1133–1137.
27. Vitola JV, Delbeke D, Sandler MP, et al. Positron emission tomography to stage suspected metastatic colorectal carcinoma to the liver. *Am J Surg.* 1996;171:21–26.
28. Lai DT, Fulham M, Stephen MS, et al. The role of whole-body positron emission tomography with [18F]fluorodeoxyglucose in identifying operable colorectal cancer metastases to the liver. *Arch Surg.* 1996;131:703–707.
29. Nagata Y, Yamamoto K, Hiraoka M, et al. Monitoring liver tumor therapy with [18F]FDG positron emission tomography. *J Comput Assist Tomogr.* 1990;14:370–374.

30. Findlay M, Young H, Cunningham D, et al. Noninvasive monitoring of tumor metabolism using fluorodeoxyglucose and positron emission tomography in colorectal cancer liver metastases: correlation with tumor response to fluorouracil. *J Clin Oncol.* 1996;4:700–708.

31. Okazumi S, Isono K, Enomoto K, et al. Evaluation of liver tumors using fluorine-18-fluorodeoxyglucose PET: characterization of tumor and assessment of effect of treatment. *J Nucl Med.* 1992;33:333–339.

32. Hamacher K, Coenen HH, Stoecklin G. Efficient stereospecific synthesis of nocarrier-added 2-[18F]-fluoro-2-deoxy-D-glucose using aminopolyether supported nucleophilic substitution. *J Nucl Med.* 1987;27:235–238.

33. Schmidlin P. Iterative Verfahren für die Emissionstomographie. *Nuklearmedizin.* 1990;3:155–158.

34. Hustinx R, Paulus P, Benoit T, Jerusalem G, Jacquet N, Rigo P. Clinical value of whole-body FDG-PET in the detection of liver metastases: preliminary results [abstract]. *Eur J Nucl Med.* 1996;23:1110.

35. Delbeke D, Vitola JV, Sandler MP, et al. Staging recurrent metastatic colorectal carcinoma with PET. *J Nucl Med.* 1997;38:1196–1201.

36. Zasadny KR, Wahl RL. Enhanced FDG-PET tumor imaging with correlation-coefficient filtered influx-constant images. *J Nucl Med.* 1996;37:371–374.

37. Tahara T, Ichiya Y, Kuwabara Y, et al. High [18F]-fluorodeoxyglucose uptake in abdominal abscesses: a PET study. *J Comput Assist Tomogr.* 1989;13:829–831.

38. Kubota R, Yamada S, Kubota K, Ishiwata K, Tamahashi N, Ido T. Intratumoral distribution of fluorine-18-fluorodeoxyglucose in vivo: high accumulation in macrophages and granulation tissues studied by microautoradiography. *J Nucl Med.* 1992;33:1972–1980.